Superresolution of color image and demosaicing

S.D.Shinde,Meeta Dewangan
Mtech(CSE)CSIT,CSVTU,Bhilai.

Asst.Prof.CSIT,CSVTU,Bhilai.

Abstract

Although the performance of imaging sensors is constantly improving, there are still several physical and practical constraints that limit the final image quality. In the last two decades, two related categories of problems have been studied independently in the image restoration literature: super-resolution and demosaicing. A closer look at these problems reveals the relation between them, and as conventional color digital cameras suffer from both low-spatial resolution and color-filtering, it is reasonable to address them in a unified context. In this paper, we propose a fast and robust hybrid method of super-resolution and demosaicing, based on a MAP estimation technique by minimizing a multi-term cost function. Finally we show that the minimization of the total cost function is relatively easy and fast. Experimental results on synthetic and real data sets confirm the effectiveness of our method.

1. Introduction

There is a growing interest in the multi-frame image reconstruction algorithms that compensate for the shortcomings of the imaging system. Such methods can achieve high-quality images using less expensive imaging chips and optical components by capturing multiple images and fusing them.

In digital photography, two image reconstruction problems have been studied and solved independently - super-resolution (SR) and demosaicing. The former refers to the limited number of pixels and the desire to go beyond this limit using several exposures. The latter refers to the color-filtering applied on a single CCD array of sensors on most cameras, that measures a subset of R (red), G (green), and B (blue) values, instead of a full RGB field. It is natural to consider these problems in a joint setting because both refer to resolution limitations at the camera. Also, since the measured images are mosaiced, solving the super-resolution problem using pre-processed (demosaiced) images is sub-optimal and hence inferior to a single unifying solution framework. In this paper we propose a fast and robust method for joint multi-frame demosaicing and color super-resolution**.**

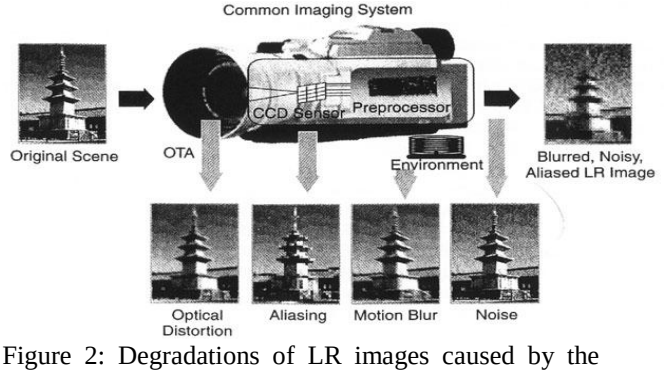

Figure 2: Degradations of LR images caused by the recording process

This paper contains review of super-resolution and demosaicing problems and the inefficiency of independent solutions for them. In another section we formulate and analyze a general model for imaging systems applicable to various scenarios of multi-frame image reconstruction. We also formulate and review the basics of the maximum a posterior (MAP) estimator, robust data fusion, and regularization methods. Armed with material developed in earlier sections, in next we present and formulate our joint multi-frame demosaicing and color-super-resolution method. After that we review two related methods of multi-frame demosaicing. Simulations on both synthetic and real data sequences are given in Section VI and concluding and implementation remarks are drawn in Section VII.

2. Review

The super resolution restoration idea was first presented by Tsay and Huang . They used the frequency domain approach to demonstrate the ability to reconstruct one improved resolution image from several down sampled noise-free versions of it, based on the spatial aliasing effect. Other results suggested a simple generalization of the above idea to noisy and blurred images. A frequency domain recursive algorithm for the restoration of super resolution images

from noisy and blurred measurements is suggested . A spatial domain alternative, based on Papoulis and Yen generalized sampling theorems is suggested by Ur and Gross . Srinivas and Srinath proposed a super resolution restoration algorithm based on a minimum mean squared error (MMSE) approach for the multiple image restoration problem and interpolation of the restored images into one. All the above super resolution restoration methods are restricted to global uniform translational displacement between the measured images, linear space-invariant (LSI) blur, and homogeneous additive noise.

A. Super-Resolution

Digital cameras have a limited spatial resolution, dictated by their utilized optical lens and CCD array. Surpassing this limit can be achieved by acquiring and fusing several low-resolution (LR) images of the same scene, producing high-resolution (HR) images; this is the basic idea behind super-resolution techniques [1], [2], [3], [4]. In the last two decades a variety of super-resolution methods have been proposed for estimating the HR image from a set of LR images. Early works on SR showed that the aliasing effects in the LR images enable the recovery of the high-resolution (HR) fused image, provided that a relative sub-pixel motion exists between the under-sampled input images [5]. However, in contrast to the clean and practically naïve frequency domain description of SR in that early work, in general SR is a computationally complex and numerically ill-behaved problem in many instances [6]. In recent years more sophisticated SR methods were developed (See [3], [6], [7], [8], [9], [10] as representative works).
Note that almost all super-resolution methods to date have been designed to increase the resolution of a single channel (monochromatic) image. A related problem, color SR, addresses fusing a set of previously demosaiced color LR frames to enhance their spatial resolution. To date, there is very little work addressing the problem of color SR. The typical solution involves applying monochromatic SR algorithms to each of the color channels independently [11], [12], while using the color information to improve the accuracy of motion estimation. Another approach is transforming the problem to a different color space, where chrominance layers are separated from luminance, and SR is applied only to the luminance channel [7]. Both of these methods are sub-optimal as they do not fully exploit the correlation across the color bands.

B. Demosaicing

A color image is typically represented by combining three separate monochromatic images. Ideally, each pixel reflects three data measurements; one for each of the color bands. In practice, to reduce production cost, many digital cameras have only one color measurement (red, green, or blue) per pixel. The detector array is a grid of CCDs, each made sensitive to one color by placing a color-filter array (CFA) in front of the CCD. The Bayer pattern shown on the left hand side of Figure 3 is a very common example of such a color-filter. The values of the missing color bands at every pixel are often synthesized using some form of interpolation from neighboring pixel values. This process is known as color *demosaicing*.
Numerous demosaicing methods have been proposed through the years to solve this under-determined problem, and in this section we review some of the more popular ones. Of course, one can estimate the unknown pixel values by linear interpolation of the known ones in each color band independently. This approach will ignore some important information about the correlation between the color bands and will result in serious color artifacts. Note that the Red and Blue channels are down-sampled two times more than the Green channel. It is reasonable to assume that the independent interpolation of the Green band will result in a more reliable reconstruction than the Red or Blue bands. This property, combined with the assumption that the *Red Green* and *Blue Green* ratios are similar for the neighboring pixels, make the basics of the smooth hue transition method first discussed in [13].
Note that there is a negligible correlation between the values of neighboring pixels located on the different sides of an edge. Therefore, although the smooth hue transition assumption is logical for smooth regions of the reconstructed image, it is not successful in the high-frequency (edge) areas. Considering this fact, gradient-based methods, first addressed in [14], do not perform interpolation across the edges of an image. This non-iterative method uses the second derivative of the Red and Blue channels to estimate the edge direction in the Green channel. Later, the Green channel is used to compute the missing values in the Red and Blue channels.
A variation of this method was later proposed in [15], where the second derivative of the Green channel and the first derivative of the Red (or Blue) channels are used to estimate the edge direction in the Green channel. The smooth hue and gradient based methods were later combined in [44]. In this iterative method, the smooth hue interpolation is done with respect to the local gradients computed in eight directions about a pixel of interest. A second stage using anisotropic inverse diffusion will further enhance the quality of the

reconstructed image. This two step approach of interpolation followed by an enhancement step has been used in many other publications. In [16], spatial and spectral correlations among neighboring pixels are exploited to define the interpolation step, while adaptive median filtering is used as the enhancement step. A different iterative implementation of the median filters is used as the enhancement step of the method described in [17], that take advantage of a homogeneity assumption in the neighboring pixels.

Iterative MAP methods form another important category of demosaicing methods. A MAP algorithm with a smooth chrominance prior is discussed in [18]. The smooth chrominance prior is also used in [19], where the original image is transformed to YIQ representation. The chrominance interpolation is preformed using isotropic smoothing. The luminance interpolation is done using edge directions computed in a steerable wavelet pyramidal structure. Other examples of popular demosaicing methods available in published literature are [20], [21], [22], [23], [24], [25], and [26]. Almost all of the proposed demosaicing methods are based on one or more of these following assumptions:

1) In the constructed image with the demosaicing pattern, there are more green sensors with regular pattern of distribution than blue or red ones (in the case of Bayer CFA there are twice as many greens than red or blue pixels and each is surrounded by 4 green pixels).
2) Most algorithms assume a Bayer CFA pattern, for which each red, green and blue pixel is a neighbor to pixels of different color bands.
3) For each pixel one and only one color band value is available.
4) The pattern of pixels does not change through the image.
5) The human eye is more sensitive to the details in the luminance component of the image than the details in chrominance component [19].
6) The human eye is more sensitive to chromatic changes in the low spatial frequency region than the luminance change [23].
7) Interpolation should be preformed along and not across the edges.
8) Different color bands are correlated with each other.
9) Edges should align between color channels.

Note that even the most popular and sophisticated demosaicing methods will fail to produce satisfactory results when severe aliasing is present in the color-filtered image. Such severe aliasing happens in cheap commercial still or video digital cameras, with small number of CCD pixels. The color artifacts worsen as the number of CCD pixels decreases. The following example shows this effect. Figure 3.a shows a HR image captured by a 3-CCD camera. If for capturing this image, instead of a 3-CCD camera a 1-CCD camera with the same number of CCD pixels was used, the inevitable demosaicing process will result in color artifacts. Figure 3.d shows the result of applying demosaicing method of [44] with some negligible color-artifacts on the edges. Note that many commercial digital video cameras can only be used in lower spatial resolution modes while working in higher frame rates. Figure 3.b shows a same scene from a 3-CCD camera with a down sampling factor of 4 and Figure 3.e shows the demo saiced image of it after color-filtering. Note that the color artifacts in this image are much more evident than 3.d. These color artifacts may be reduced by low-pass filtering the input data before color-filtering. Figure 3.c shows a factor of four down-sampled version of 3.a, which is blurred with a symmetric Gaussian low-pass filter of size 4×4 with standard deviation equal to one, before down-sampling. The demo saiced image shown in 3.f has less color artifacts than 3.e, however it has lost some high-frequency details. The poor quality of single-frame demosaiced images stimulates us to search for multi-frame demosaicing methods, where the information of several low-quality images are fused together to produce high-quality demosaiced images.

C. Merging super-resolution and demosaicing into one process

Referring to the mosaic effects, the geometry of the single-frame and multi-frame demosaicing problems are fundamentally different, making it impossible to simply cross apply traditional demosaicing algorithms to the multi-frame situation. To better understand the multi-frame demosaicing problem, we offer an example for the case of translational motion. Suppose that a set of color-filtered LR images is available (images on the left in Figure 4). We use the two step process explained in Section IV to fuse these images. The Shift-And-Add image on the right side of Figure 3 illustrates the pattern of sensor measurements in the HR image grid. In such situations, the sampling pattern is quite arbitrary depending on the relative motion of the LR images. This necessitates different demosaicing algorithms than those designed for the original Bayer pattern.


a: Original


b: Down-sampled


c: Blurred and down-sampled


d: Demosaiced (a)


e: Demosaiced (b)


f: Demosaiced (c)

Fig. 3. A HR image (a) captured by a 3-CCD camera is down-sampled by a factor of four (b). In (c) the image in (a) is blurred by a Gaussian kernel before down-sampling by a factor of 4. The images in (a), (b), and (c) are color-filtered and then demosaiced by the method of [44]. The results are shown in (d), (e), (f), respectively.

Figure 4 shows that treating the green channel differently than the red or blue channels, as done in many single-frame demosaicing methods before, is not useful for the multi-frame case. While globally there are more green pixels than blue or red pixels, locally, any pixel may be surrounded by only red or blue colors. So, there is no general preference for one color band over the others (the first and second assumptions in Section II-B are not true for the multi-frame case). Another assumption, the availability of one and only one color band value for each pixel, is also not correct in the multi-frame case. In the under-determined cases , there are not enough measurements to fill the HR grid. The symbol "?" in Figure 4 represents such pixels. On the other hand, in the over-determined cases6, for some pixels, there may in fact be more than one color value available. The fourth assumption in the existing demosaicing literature described earlier is not true because the field of view (FOV) of real world LR images changes from one frame to the other, so the center and the border patterns of red, green, and blue pixels differ in the resulting HR image.

3.Mathematical model and solution outline

A. Mathematical Model of the Imaging System

Figure 1 illustrates the image degradation model that we consider. We represent this approximated forward model by the following equation:

$$Y\,i(k) = Di(k)H(k)F(k)Xi + V\,i(k) = Ti(k)Xi + V\,i(k)\ k = 1, \ldots, N$$

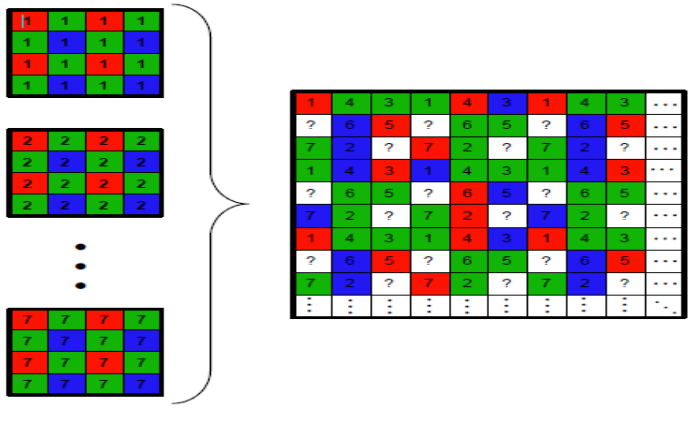

Fig. 4. Fusion of 7 Bayer pattern LR images with relative translational motion (the figures in the left side of the accolade) results in a HR image (_*Z*) that does not follow Bayer pattern (the figure in the right side of the accolade). The symbol "?" represents the HR pixel values that were undetermined (as a result of insufficient LR frames) after the Shift-And-Add step

(Shift-And-Add method is extensively discussed in [3], and briefly reviewed in III-F).

$i = R,G,B$, (1)

which can be also expressed as:

$Y = TX + V$,

$$Y=\begin{vmatrix} Y\,R(1) \\ Y\,G(1) \\ Y\,B(1) \\ Y\,R(2) \\ \ldots \\ Y\,B(N) \end{vmatrix} \qquad V=\begin{vmatrix} VR(1) \\ VG(1) \\ V\,B(1) \\ V\,R(2) \\ \ldots. \\ VB(N) \end{vmatrix}$$

$$T=\begin{vmatrix} TR(1) \\ TG(1) \\ TB(1) \\ TR(2) \\ \ldots \\ TB(N) \end{vmatrix} \qquad X=\begin{vmatrix} XR \\ XG \\ XB \end{vmatrix} \qquad (2)$$

The vectors Xi and $Y\,i(k)$ are representing the *ith* band (R, G, or B) of the HR color frame and the *kth* LR frame after lexicographic ordering, respectively. Matrix $F(k)$ is the geometric motion operator between the HR and LR frames. The camera's point spread function (PSF) is modeled by the blur matrix $H(k)$. The matrix $Di(k)$ represents the down-sampling operator, which includes both the color-filtering and CCD down-sampling operations. Geometric motion, blur, and down-sampling operators are covered by the operator $Ti(k)$, which we call the system matrix. The vector $V\,i(k)$ is the system noise and N is the number of available LR frames.

The HR color image (X) is of size [12r2M2 ×1]), where r is the resolution enhancement factor. The size of the vectors $V\,G(k)$ and $Y\,G(k)$ is [2M2×1] and vectors $V\,R(k)$, $Y\,R(k)$, $V\,B(k)$, and $Y\,B(k)$ are of size [M2×1]. The geometric motion and blur matrices are of size [4r2M2×4r2M2]. The down-sampling and system matrices are of size [2M2 × 4r2M2] for the Green band and of size [M2 × 4r2M2] for the Red and Blue bands8 Considered separately, super-resolution and demosaicing models are special cases of the general model presented above. In particular, in the super-resolution literature the effect of color-filtering is usually ignored [9], [10], [3] and therefore the model is simplified to:

$$Y\,(k) = D(k)H(k)F(k)X + V\,(k)\ k = 1, \ldots ,N\,. \qquad (3)$$

In this model the LR images $Y\,(k)$ and the HR image X are assumed to be monochromatic. On the other hand, in the demosaicing literature only single frame reconstruction of color images is considered, resulting in a simplified model:

$$Y\,i = DiXi + V\,i\ i = R,G,B\,. \quad (4)$$

As such, the classical approach to the multi-frame reconstruction of color images has been a two-step process. The first step is to solve (4) for each image (demosaicing step) and the second step is to use the model in (3) to fuse the LR images resulting from the first step, reconstructing the color HR image (usually each R, G , or B bands is processed individually). Of course, this two step method is a suboptimal approach to solving the overall problem. In Section IV, we propose a Maximum A-Posteriori (MAP) estimation approach to directly solve (1).

B. MAP Approach to Multi-Frame Image Reconstruction

Following the forward model of (1), the problem of interest is an inverse problem, wherein the source of information (HR image) is estimated from the observed data (LR images). An inherent difficulty with inverse problems is the challenge of inverting the forward model without amplifying the effect of noise in the measured data. In many real scenarios, the problem is worsened by the fact that the system matrix T is singular or ill-conditioned. Thus, for the problem of super-resolution, some form of regularization must be included in the cost function to stabilize the problem or constrain the space of solutions. From a statistical perspective, regularization is incorporated as *a priori* knowledge about the solution. Thus, using the Maximum A-Posteriori (MAP) estimator, a rich class of regularization functions emerges, enabling us to capture the specifics of a particular application. This can be accomplished by way of Lagrangian type penalty terms as in

$$X = \text{ArgMin}\ X[\rho(Y\ ,\ TX) + \lambda\Gamma(X)]\ , \quad (5)$$

where ρ, the data fidelity term, measures the "distance" between the model and measurements, and Γ is the regularization cost function, which imposes a penalty on the unknown X to direct it to a better formed solution. The regularization parameter, λ, is a scalar for properly weighting the first term (data fidelity cost) against the second term (regularization cost). Generally speaking, choosing λ could be either done manually, using visual inspection, or automatically using methods like Generalized Cross Validation[28], [29], L-curve [30], or other techniques.

4. Related work

Although their method has produced successful results for the single frame demosaicing problem, it is not specifically posed or directed towards solving the multi-frame demosaicing problem, and no multi-frame demosaicing case experiment is given. To estimate the Red channel, first, affine relations that project Green and Blue channels to the Red channel are computed. In

the second stage, a super-resolution algorithm (e.g. the method of [7]) is applied on the available LR images in the Red channel (i.e. the original CFA data of the Red channel plus the projected Green and Blue channels) to estimate the HR Red channel image. A similar procedure estimates the HR Green and Blue channel images. As affine model is not always valid for all sensors or image sets, so an affine model validity test is utilized in [38]. In the case that the affine model is not valid for some pixels, those projected pixels are simply ignored. The method of [38] is highly dependent on the validity of the affine model, which is not confirmed for the multi-frame case with inaccurate registration artifacts. Besides, the original CFA LR image of a channel and the less reliable projected LR images of other channels are equally weighted to construct the missing values, and this does not appear to be an optimal solution.

In contrast to their method, our proposed technique exploits the correlation of the information in different channels explicitly to guarantee similar edge position and orientation in different color bands. Our proposed method also exploits the difference in sensitivity of the human eye to the frequency content and outliers in the luminance and chrominance components of the image.

5.EXPERIMENTS

Experiments on synthetic and real data sets are presented in this section. In the first experiment, following the model of (1), we created a sequence of LR frames from an original HR image , which is a color image with full RGB values. First we shifted this HR image by one pixel in the vertical direction. Then to simulate the effect of camera PSF, each color band of this shifted image was convolved with a symmetric Gaussian low-pass filter of size 5 × 5 with standard deviation equal to one. The resulting image was sub sampled by the factor of 4 in each direction. The same process with different motion vectors (shifts) in vertical and horizontal directions was used to produce 10 LR images from the original scene. The horizontal shift between the low resolution images was varied between 0 to .75 pixels in the low-resolution grid (0 to 3 pixels in the high-resolution grid). The vertical shift between the low resolution images varied between 0 to .5 pixels in the low-resolution grid (0 to 2 pixels in the high-resolution grid). To simulate the errors in motion estimation, a bias equal to half a pixel shift in the LR grid was intentionally added to the known motion vector of one of the LR frames. We added Gaussian noise to the resulting LR frames to achieve SNR equal12 to 30dB. Then each LR color image was sub sampled by the Bayer filter.

6. DISCUSSION AND FUTURE WORK

In this paper, based on the MAP estimation framework, we proposed a unified method of demosaicing and super-resolution, which increases the spatial resolution and reduces the color artifacts of a set of low quality color images. Using the $L1$ norm for the data error term makes our method robust to errors in data and modelling. Bilateral regularization of the luminance term results in sharp reconstruction of edges, and the chrominance and inter-color dependencies cost functions remove the color artifacts from the HR estimate. All matrix-vector operations in the proposed method are implemented as simple image operators. As these operations are locally performed on pixel values on the HR grid, parallel processing may also be used to further increase the computational efficiency. The computational complexity of this method is on the order of the computational complexity of the popular iterative super-resolution algorithms, such as [9]. Namely, it is linear in the number of pixels.

Accurate subpixel motion estimation is an essential part of any image fusion process such as multiframe super-resolution or demosaicing. To the best of our knowledge, no paper has addressed the problem of estimating motion between Bayer filtered images.

REFERENCES

[1] S. Borman and R. L. Stevenson, “Super-resolution from image sequences - a review,” in *Proc. of the 1998 Midwest Symposium on Circuits and Systems*, vol. 5, Apr. 1998.

[2] S. Park, M. Park, and M. G. Kang, “Super-resolution image reconstruction, a technical overview,” *IEEE Signal Processing Magazine*, vol. 20, no. 3, pp. 21–36, May 2003.

[3] S. Farsiu, D. Robinson, M. Elad, and P. Milanfar, “Fast and robust multi-frame super-resolution,” *IEEE Trans. Image Processing*, vol. 13, no. 10, pp. 1327–1344, Oct. 2004.

[4] ——, “Advances and challenges in super-resolution,” *International Journal of Imaging Systems and Technology*, vol. 14, no. 2, pp. 47–57, Aug. 2004.

[5] T. S. Huang and R. Y. Tsai, “Multi-frame image restoration and registration,” *Advances in computer vision and Image Processing*, vol. 1, pp. 317–339, 1984.

[6] N. Nguyen, P. Milanfar, and G. H. Golub, “A computationally efficient image superresolution algorithm,” *IEEE Trans. Image Processing*, vol. 10, no. 4, pp. 573–583, Apr. 2001.

[7] M. Irani and S. Peleg, "Improving resolution by image registration," *CVGIP:Graph. Models Image Process*, vol. 53, pp.
231–239, 1991.
[8] S. Peleg, D. Keren, and L. Schweitzer, "Improving image resolution using subpixel motion," *CVGIP:Graph. Models Image Processing*, vol. 54, pp. 181–186, March 1992.
[9] M. Elad and A. Feuer, "Restoration of single super-resolution image from several blurred, noisy and down-sampled
measured images," *IEEE Trans. Image Processing*, vol. 6, no. 12, pp. 1646–1658, Dec. 1997.
[10] A. Zomet and S. Peleg, "Efficient super-resolution and applications to mosaics," in *Proc. of the Int. Conf. on Pattern
Recognition (ICPR)*, Sept. 2000, pp. 579–583.
[11] N. R. Shah and A. Zakhor, "Resolution enhancement of color video sequences," *IEEE Trans. Image Processing*, vol. 8,
no. 6, pp. 879–885, June 1999.
[12] B. C. Tom and A. Katsaggelos, "Resolution enhancement of monochrome and color video using motion compensation,"
IEEE Trans. Image Processing, vol. 10, no. 2, pp. 278–287, Feb. 2001.
[13] D. R. Cok, "Signal processing method and apparatus for sampled image signals," United States Patent 4,630,307, 1987.
[14] C. Laroche and M. Prescott, "Apparatus and method for adaptively interpolating a full color image utilizing chrominance
gradients," United States Patent 5,373,322, 1994.
[15] J. Hamilton and J. Adams, "Adaptive color plan interpolation in single sensor color electronic camera," United States
Patent 5,629,734, 1997.
[16] L. Chang and Y.-P. Tan, "Color filter array demosaicking: new method and performance measures," *IEEE Trans. Image
Processing*, vol. 12, no. 10, pp. 1194–1210, Oct. 2002.
[17] K. Hirakawa and T. Parks, "Adaptive homogeneity-directed demosaicing algorithm," in *Proc. of the IEEE Int. Conf. on
Image Processing*, vol. 3, Sept. 2003, pp. 669–672.
[18] D. Keren and M. Osadchy, "Restoring subsampled color images," *Machine Vision and applications*, vol. 11, no. 4, pp.
197–202, 1999.
26
[19] Y. Hel-Or and D. Keren, "Demosaicing of color images using steerable wavelets," HP Labs Israel, Tech. Rep.
HPL-2002-206R1 20020830, 2002. [Online]. Available: citeseer.nj.nec.com/548392.html
[20] D. Taubman, "Generalized Wiener reconstruction of images from colour sensor data using a scale invariant prior," in *Proc.
of the IEEE Int. Conf. on Image Processing*, vol. 3, Sept. 2000, pp. 801–804.
[21] D. D. Muresan and T. W. Parks, "Optimal recovery demosaicing," in *IASTED Signal and Image Processing*, Aug. 2002.
[22] B. K. Gunturk, Y. Altunbasak, and R. M. Mersereau, "Color plane interpolation using alternating projections," *IEEE Trans.
Image Processing*, vol. 11, no. 9, pp. 997–1013, Sep. 2002.
[23] S. C. Pei and I. K. Tam, "Effective color interpolation in CCD color filter arrays using signal correlation," *IEEE Trans.
Image Processing*, vol. 13, no. 6, pp. 503–513, June 2003.
[24] D. Alleysson, S. S¨usstrunk, and J. Hrault, "Color demosaicing by estimating luminance and opponent chromatic signals
in the Fourier domain," in *Proc. of the IS&T/SID 10th Color Imaging Conf.*, Nov. 2002, pp. 331–336.
[25] X. Wu and N. Zhang, "Primary-consistent soft-decision color demosaic for digital cameras," in *Proc. of the IEEE Int.
Conf. on Image Processing*, vol. 1, Sept. 2003, pp. 477–480.
[26] R. Ramanath and W. Snyder, "Adaptive demosaicking," *Journal of Electronic Imaging*, vol. 12, no. 4, pp. 633–642, Oct.
2003.
[27] S. Farsiu, M. Elad, and P. Milanfar, "Multi-frame demosaicing and super-resolution from under-sampled color images,"
Proc. of the 2004 IS&T/SPIE Symp. on Electronic Imaging, vol. 5299, pp. 222–233, Jan. 2004.
[28] M. A. Lukas, "Asymptotic optimality of generalized cross-validation for choosing the regularization parameter," *Numerische
Mathematik*, vol. 66, no. 1, pp. 41–66, 1993.
[29] N. Nguyen, P. Milanfar, and G. Golub, "Efficient generalized cross-validation with applications to parametric image
restoration and resolution enhancement," *IEEE Trans. Image Processing*, vol. 10, no. 9, pp. 1299–1308, Sept. 2001.
[30] P. C. Hansen and D. P. O'Leary, "The use of the L-curve in the regularization of ill-posed problems," *SIAM J. Sci. Comput.*,
vol. 14, no. 6, pp. 1487–1503, Nov. 1993.

[31] L. Rudin, S. Osher, and E. Fatemi, "Nonlinear total variation based noise removal algorithms," *Physica D*, vol. 60, pp. 259–268, Nov. 1992.
[32] T. F. Chan, S. Osher, and J. Shen, "The digital TV filter and nonlinear denoising," *IEEE Trans. Image Processing*, vol. 10, no. 2, pp. 231–241, Feb. 2001.
[33] C. Tomasi and R. Manduchi, "Bilateral filtering for gray and color images," in *Proc. of IEEE Int. Conf. on Computer Vision*, Jan. 1998, pp. 836–846.
[34] M. Elad, "On the bilateral filter and ways to improve it," *IEEE Trans. Image Processing*, vol. 11, no. 10, pp. 1141–1151, Oct. 2002.
[35] M. E. Tipping and C. M. Bishop, "Bayesian image super-resolution," *Advances in Neural Information Processing Systems*, vol. 15, pp. 1303–1310, 2002.
[36] S. Farsiu, D. Robinson, M. Elad, and P. Milanfar, "Robust shift and add approach to super-resolution," *Proc. of the 2003 SPIE Conf. on Applications of Digital Signal and Image Processing*, pp. 121–130, Aug. 2003.
[37] W. K. Pratt, *Digital image processing*, 3rd ed. New York: John Wiley & Sons, INC., 2001.
[38] A. Zomet and S. Peleg, "Multi-sensor super resolution," in *Proc. of the IEEE Workshop on Applications of Computer Vision*, Dec. 2001, pp. 27–31.
[39] T. Gotoh and M. Okutomi, "Direct super-resolution and registration using raw CFA images," in *Proc. of the Int. Conf. on Computer Vision and Pattern Recognition (CVPR)*, vol. 2, July 2004, pp. 600–607.